ANTITUMOR IMMUNITY

A shed NKG2D ligand that promotes natural killer cell activation and tumor rejection

Weiwen Deng,[1] Benjamin G. Gowen,[1] Li Zhang,[1] Lin Wang,[1] Stephanie Lau,[1] Alexandre Iannello,[1] Jianfeng Xu,[1] Tihana L. Rovis,[2] Na Xiong,[3] David H. Raulet[1]*

Immune cells, including natural killer (NK) cells, recognize transformed cells and eliminate them in a process termed immunosurveillance. It is thought that tumor cells evade immunosurveillance by shedding membrane ligands that bind to the NKG2D-activating receptor on NK cells and/or T cells, and desensitize these cells. In contrast, we show that in mice, a shed form of MULT1, a high-affinity NKG2D ligand, causes NK cell activation and tumor rejection. Recombinant soluble MULT1 stimulated tumor rejection in mice. Soluble MULT1 functions, at least in part, by competitively reversing a global desensitization of NK cells imposed by engagement of membrane NKG2D ligands on tumor-associated cells, such as myeloid cells. The results overturn conventional wisdom that soluble ligands are always inhibitory and suggest a new approach for cancer immunotherapy.

Natural killer (NK) cells and some T cells use activating receptors such as NKG2D to recognize and eliminate infected and transformed cells that up-regulate ligands for these receptors (*1*). There are six to eight different NKG2D ligands, which are poorly expressed by normal cells but up-regulated in cancer cells (*2*). Many tumor cells release soluble NKG2D ligands through proteolytic shedding, alternative splicing, or exosome secretion (*2*, *3*). Numerous reports conclude that excreted NKG2D ligands modulate NKG2D from the cell surface and desensitize antitumor effector cells (*4*, *5*), although a functional impact of soluble NKG2D ligands is not always observed (*6*–*9*). To study shed NKG2D ligands in a controlled setting, we focused on the mouse ligand MULT1, which is commonly up-regulated in primary tumors (*10*) and is a transmembrane protein, as are the human ligands major histocompatibility complex (MHC) class I chain–related protein A (MICA), MICB, ULBP4, and ULBP5 (*11*). Analysis of fibroblasts transduced with either N- or C-terminally tagged MULT1 revealed an N-terminal species (23 kD after deglycosylation) shed into the culture supernatant (fig. S1A) and a 24 kD membrane "stub" in the cell lysates, in addition to full-length (around 42 kD) MULT1 (fig. S1B). Inhibiting matrix metalloproteinases blocked MULT1 shedding (fig. S1C).

Hemagglutinin (HA)–MULT1–transduced fibroblasts produced nearly eightfold more shed MULT1 than did untransduced fibroblasts (fig. S2). WEHI-7.1 and C1498 but not human 293T cell lines excreted MULT1 produced endogenously. We detected serum MULT1 (mean concentration ~250 ng/ml) in most tumor-bearing *Eμ-myc* transgenic mice, which frequently develop MULT1$^+$ tumors (*10*), but not in most nontransgenic littermates (Fig. 1A). Very high concentrations of soluble MULT1 were also detected in sera of *Apoe*$^{-/-}$ mice fed a high-fat diet (Fig. 1A). Given that atherosclerosis and liver inflammation in such mice are largely dependent on NKG2D function (*12*), it seemed unlikely that soluble MULT1 inhibits NKG2D function. Thus, MULT1 is released from cell lines that naturally or ectopically express MULT1 and accumulates in sera of animals with spontaneous tumors and NKG2D-dependent inflammatory disease.

Purified shed HA-MULT1 bound to NKG2D with high affinity [average dissociation constant (K_d) of 13 ± 3.8 nM] (fig. S3), similar to the affinity reported for recombinant MULT1 (*13*). In parallel, we engineered fibroblasts to secrete an ectodomain fragment of HA-MULT1 (which we call "secMULT"). SecMULT1 also bound to NKG2D with high affinity (19 ± 4.3 nM) (fig. S3).

To test the function of soluble MULT1, we engineered two NKG2D ligand-negative B6 strain tumor cell lines (the B16-BL*6* melanoma and RMA lymphoma) to secrete secMULT1. Surprisingly, both cell lines were rejected by syngeneic B6 mice compared with cells transduced with empty vector (Fig. 1B and fig. S4A), despite the absence of cell surface MULT1 (fig. S4B). Tumor cells transduced with full-length MULT1 [mutated in the cytoplasmic tail to optimize cell surface expression (fig. S4B) (*14*)] were also rejected (Fig. 1B). B16-secMULT1 cells were still rejected in B6 hosts that had been depleted of CD8$^+$ cells but grew progressively in B6 and *Rag1*$^{-/-}$ hosts that had been depleted of NK1.1$^+$ cells (Fig. 1C and fig. S5). Hence, NK cells but not CD8$^+$ cells participate in the rejection of B16-secMULT1. B16 cells with inducible secMULT1 (fig. S6) were also partially rejected (Fig. 1D). In this case, the secMULT1 lacked an epitope tag, showing that rejection occurs without a tag. A mixture of B16 (90%) and B16-secMULT1 (10%) cells was also rejected, demonstrating that sec-MULT1 acts extrinsically (Fig. 1E). These data ruled out the possibility that rejection was solely due to intrinsic stress responses in sec-MULT1–expressing tumor cells. Instead, the data suggested that secMULT1 mobilizes or activates antitumor effector cells.

To address whether tumor cells secreting secMULT1 activate NK cells, we adapted a short-term in vivo NK induction protocol (*15*, *16*) by injecting irradiated tumor cells intraperitoneally in normal mice. Injection of B16-secMULT1 or B16 cells induced similar modest increases in the percentages of NK cells in the peritoneal washes 3 days later (fig. S7), but B16-secMULT1 cells induced more potent ex vivo killing activity against NK-sensitive YAC-1 tumor cells (Fig. 2A). Similar results were obtained with RMA-secMULT1 cells (fig. S8A). Furthermore, higher percentages of peritoneal NK cells from mice injected with B16-secMULT1 cells produced interferon-γ (IFN-γ) after stimulation ex vivo with YAC-1 tumor cells (Fig. 2B) or immobilized antibodies against NK-activating receptors (Fig. 2C and fig. S8B). To allow the recovery of intratumoral NK cells at early times after subcutaneous transfer, we implanted 3×10^5 to 5×10^5 tumor cells mixed with matrigel. Seven days later, NK cells extracted from B16-secMULT1 tumors exhibited stronger IFN-γ responses after stimulation ex vivo (Fig. 2D). Therefore, soluble MULT1 stimulated NK cell functional capacities in both subcutaneous and peritoneal tumors.

Recombinant MULT1 (rMULT1) is similar in size to shed MULT1. When injected with B16 tumor cells (fig. S9A), rMULT1 resulted in partial tumor rejection (Fig. 2E and fig. S9B), and NK cells extracted from the tumors exhibited increased functional activity after stimulation ex vivo (Fig. 2F). The rMULT1 sample was devoid of endotoxin or other PAMPs that activate macrophages (fig. S9C). These data established that soluble MULT1 causes tumor rejection, likely by activating NK cells.

secMULT1 and shed MULT1 are monomeric (fig. S10, A to C) and should not cross-link NKG2D, which is typically necessary for immune receptor activation. Indeed, monomeric rMULT1 failed to stimulate IFN-γ production when incubated with peritoneal NK cells for 4 hours (fig. S11A). Soluble MULT1 may form a multivalent array in vivo, but preliminary staining analyses failed to detect such arrays. These data argue that soluble MULT1 stimulates NK cells by other mechanisms.

Target cells bearing membrane NKG2D ligands, including MULT1, caused down-regulation of cell surface NKG2D, presumably by aggregating the receptor and triggering receptor endocytosis (Fig. 3A) (*8*, *17*). Tumor cells secreting secMULT1, in contrast, caused NKG2D up-regulation on

[1]Department of Molecular and Cell Biology, and Cancer Research Laboratory, University of California at Berkeley, Berkeley, CA 94720, USA. [2]Center for Proteomics University of Rijeka Faculty of Medicine Brace Branchetta 20, 51000 Rijeka, Croatia. [3]Department of Veterinary and Biomedical Sciences, Pennsylvania State University, 115 Henning Building, University Park, PA 16802, USA.
*Corresponding author. E-mail: raulet@berkeley.edu

NK cells in vivo (Fig. 3, A and B), without affecting an irrelevant receptor, DNAM-1 (Fig. 3B). NKG2D up-regulation occurred without increases in NKG2D mRNA (fig. S12) or intracellular protein. These findings suggested the following hypothesis (Fig. 3C): that untransformed host cells express membrane NKG2D ligands that persistently engage NK cells, cause NKG2D down-regulation, and globally desensitize the NK cells as the tumors progress; and that soluble MULT1 enhances responsiveness and cell-surface NKG2D expression by blocking these interactions.

Consistent with the hypothesis, host $CD11b^{+}F4/80^{+}$ myeloid cells associated with either peritoneal or subcutaneous B16 or B16-secMULT1 tumors displayed the NKG2D ligand RAE-1 (but not MULT1) on the cell surface (Fig. 3, D and E). Monocytes in patients with several types of cancer also expressed NKG2D ligands (*18*). Tumors may cause an increase in RAE-1 expression by myeloid cells in the peritoneum (Fig. 3D) and possibly other sites (*19*). Hence, myeloid cells, and possibly other nontumor cells, express NKG2D ligands in vivo. We further demonstrated that rMULT1 competitively blocks binding of RAE-1ε-Fc fusion protein to NKG2D on NK cells (Fig. 3F), confirming a distinct prediction of the hypothesis.

To test whether RAE-1 expressed on endogenous cells caused NK cell inactivation, we used

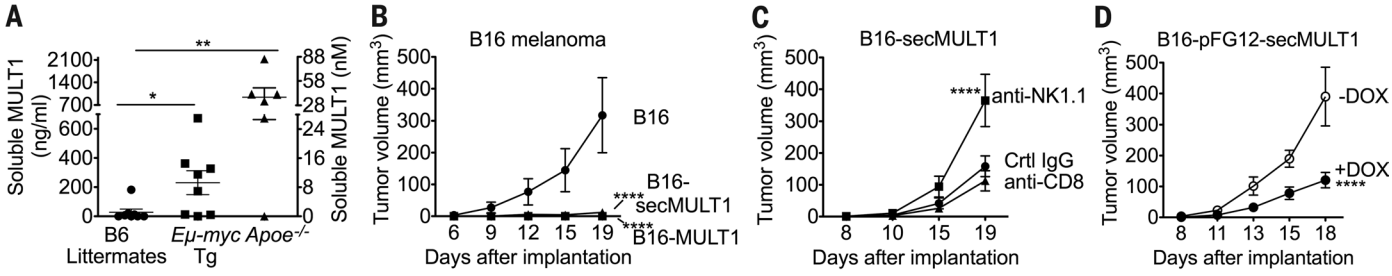

Fig. 1. NK cells promote the rejection of tumors that shed MULT1. (**A**) Enzyme-linked immunosorbent assay detection of soluble MULT1 in sera from tumor-bearing *Eμ-Myc* mice, nontransgenic littermates, and diseased *Apoe*$^{-/-}$ mice fed a Western diet (n = 6 to 8 mice). Each point represents a different mouse. (**B**) Comparison of growth of 2 × 10^4 subcutaneously transferred B16 melanoma tumor cells transduced with secMULT1, full-length MULT1, or empty vector, in wild-type (WT) B6 mice (n = 4 mice). Rejection was usually partial but was complete in some animals in some experiments. (**C**) Subcutaneous growth of B16-secMULT1 tumors in B6 mice (2 × 10^4 cells were inoculated) treated with control imuunoglobulin G (IgG), NK1.1 antibody, or CD8 antibody (n = 13 mice). (**D**) After inoculation of 2 × 10^4 B16 cells transduced with pFG12-secMULT1, mice were treated or not with doxycycline starting from the time of tumor implantation (n = 6 mice). (**E**) Mice (n = 6) received 2 × 10^4 B16 cells alone, or 2 × 10^4 B16 cells mixed with 2 × 10^3 B16-secMULT1 cells. Shown are representative examples of ≥3 [(B) and (E)] or 2 (D) experiments performed, whereas (C) includes combined data from 3 experiments. Tumor volumes ± SE are shown. (A) was analyzed with a Mann-Whitney test, and (B) to (E) were analyzed by two-way analysis of variance (ANOVA) with Bonferroni multiple comparison tests. *P < 0.05, **P < 0.01, ***P < 0.001 and ****P < 0.0001.

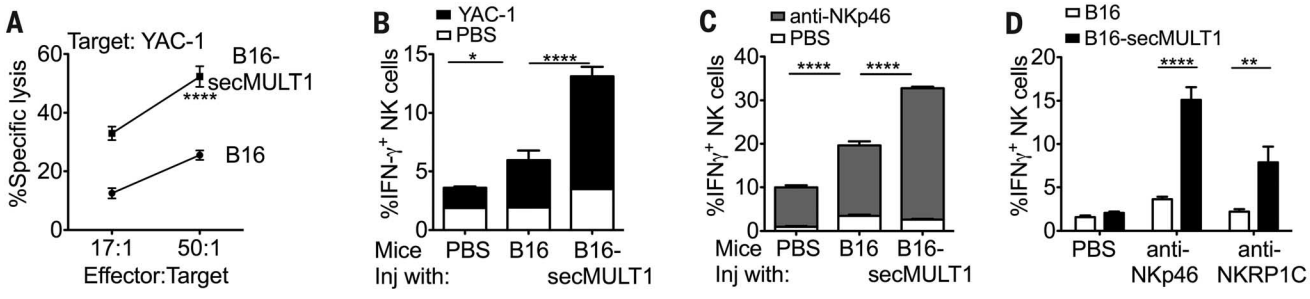

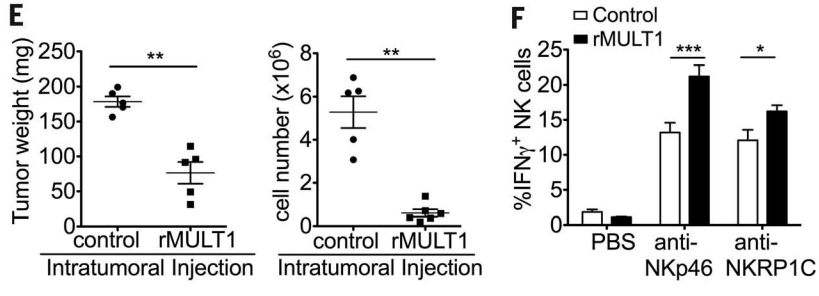

Fig. 2. Soluble MULT1 amplifies NK cell responses and causes tumor rejection. (**A** to **C**) B6 mice were injected intraperitoneally with 5 × 10^6 irradiated B16 or B16-secMULT1 cells, or phosphate-buffered saline (PBS). Peritoneal wash cells (pooled from five mice) were recovered 3 days later and tested for (A) killing of YAC-1 target cells, (B) intracellular IFN-γ after stimulation with YAC-1 cells, or (C) immobilized NKp46 antibody; control responses to PBS are depicted by white segments of the bars. (**D**) B6 mice were injected subcutaneously with 3 × 10^5 to 5 × 10^5 B16 or B16-secMULT1 cells in 100 μl matrigel. The tumors were dissociated 7 days later, and gated NK cells from individual mice (n = 5 mice) were tested for responses to immobilized NKp46 or NKRP1C Abs. (**E** and **F**) Subcutaneous tumors were established with 3 × 10^5 to 5 × 10^5 B16 cells in matrigel. The tumor cells in one group were mixed with 1 μg of recombinant MULT1 (rMULT1). After 4 days, an additional 1 μg of rMULT1 (or PBS for control mice) was injected into each matrigel/tumor for that group. On day 7, tumors were extracted, (E) weighed, dissociated, and (E) the tumor cells were counted. The immune cells within the tumors were stimulated with immobilized NKp46 and NKRP1C Abs, and (F) the IFN-γ responses of gated NK cells were determined. Shown are representative examples of 2 (A) or ≥3 [(B) to (F)] experiments performed. (A) to (D) and (F) were analyzed with two-way ANOVA with Bonferroni multiple comparison tests, (E) was analyzed with Mann-Whitney test. *P < 0.05, **P < 0.01, ***P < 0.001 and ****P < 0.0001.

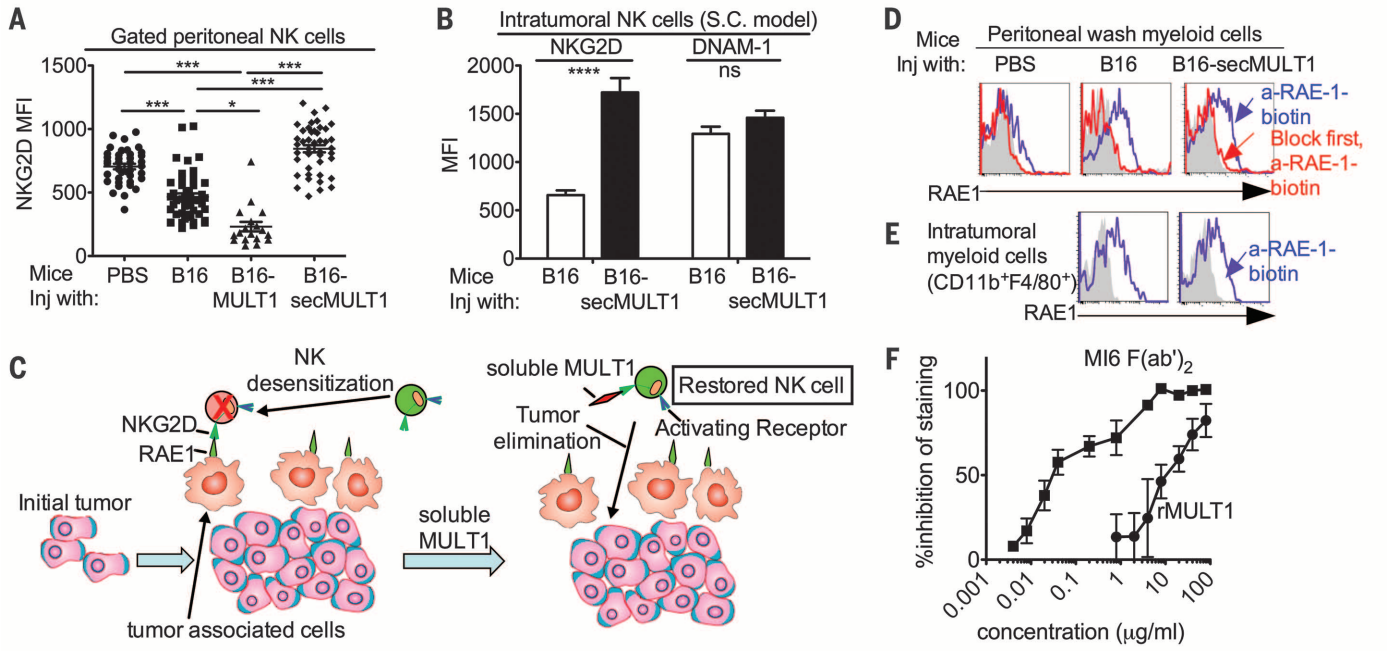

Fig. 3. Mechanisms of immune activation by soluble MULT1. (**A** and **B**) Membrane NKG2D staining after exposure of NK cells to secMULT1 in intraperitoneal (A) or subcutaneous (B) tumors. (**C**) Model of secMULT1 action. Persistent NKG2D engagement by endogenous NKG2D ligand–expressing cells associated with the tumor desensitizes NK cells. Soluble MULT1 competitively blocks the NKG2D receptor, preventing NK cell desensitization and therefore augmenting tumor rejection mediated through distinct NK-activating receptors. (**D**) Expression of NKG2D ligand RAE-1 by gated $CD11b^+F480^+$ peritoneal myeloid cells in mice injected intraperitoneally 3 days before with PBS or 5×10^6 irradiated B16 or B16-secMULT1 tumor cells. Cells were stained with biotin-pan-RAE-1 Ab (blue). The staining was specific because it could be blocked by including an excess of unconjungated pan-RAE-1 antibody in the reaction (red). Gray shows isotype control staining. (**E**) Expression of RAE-1 by gated $CD11b^+F480^+$ intratumoral myeloid cells in mice injected subcutaneously with 2×10^4 B16 or B16-secMULT1 tumor cells 20 days before. (**F**) rMULT1 and NKG2D antibody [MI6 clone, in $F(ab')_2$ form] block RAE-1 binding to NKG2D on NK cells. The mean fluorescence intensity of RAE1ε-Fc staining of NK cells was used to calculate percent inhibition. (A) is combined data from 14 experiments. (B) and (D) to (F) show representative examples of ≥3 experiments performed. (A) was analyzed with one-way ANOVA Kruskal-Wallis test, (B) was analyzed with two-way ANOVA with Bonferroni multiple comparison tests; ns indicates $P > 0.05$, $^*P < 0.05$, and $^{***}P < 0.001$.

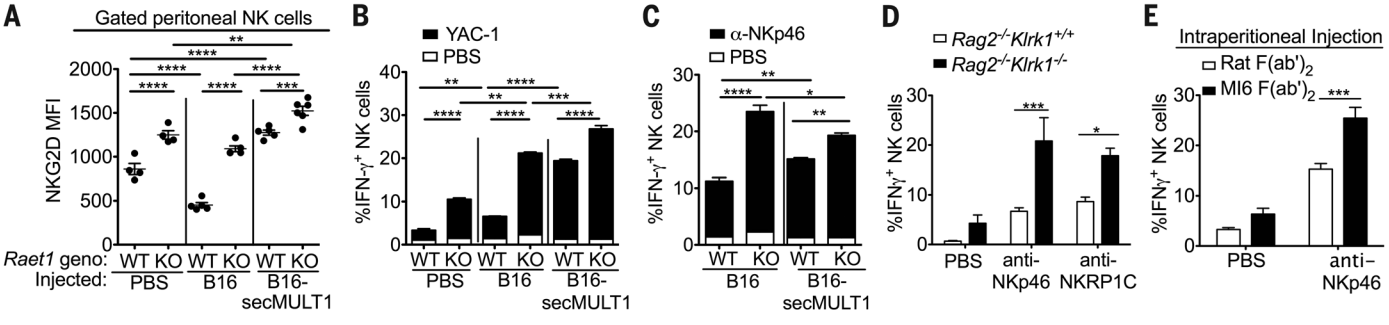

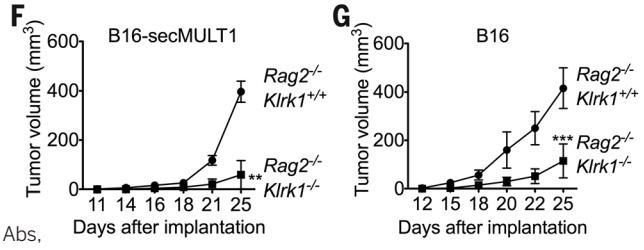

Fig. 4. Augmented NK cell responses in RAE-1–deficient and NKG2D-deficient mice. (**A** to **C**) Peritoneal NK cells from *Raet1d*$^{-/-}$*Raet1e*$^{-/-}$ mice (KO) exhibited (A) increased amounts of cell-surface NKG2D and (B) increased functional responses ex vivo to YAC-1 tumor cells or (C) NKp46 antibody stimulation; control responses to PBS are depicted by white segments of the bars. The effects were larger when the mice were injected 3 days earlier with irradiated B16 tumor cells but smaller when they were injected with B16-secMULT1 tumor cells. (**D**) NKG2D-deficient (*Klrk1*$^{-/-}$) NK cells exhibited increased functional activity. Splenic NK cells from *Rag*$^{-/-}$ and *Rag*$^{-/-}$ *Klrk1*$^{-/-}$ mice were stimulated ex vivo with immobilized NKp46 or NKRP1C Abs, and the IFN-γ responses of gated NK cells were determined. (**E**) B6 mice were injected intraperitoneally with 50 μg MI6 (anti-NKG2D) $F(ab')_2$ or $F(ab')_2$ of rat IgG on days 0, 3, and 6. On Day 8, peritoneal NK cells were stimulated ex vivo with immobilized NKp46 Abs, and the IFN-γ responses of gated NK cells were determined. (**F** and **G**) Increased tumor rejection responses in NKG2D-deficient mice. Growth of (F) B16-secMULT1 or (G) B16 tumor cells in *Rag2*$^{-/-}$ or *Rag2*$^{-/-}$*Klrk1*$^{-/-}$ mice ($n = 5$ mice). (F) and (G) are from separate experiments. Separate, direct comparisons showed retarded growth of B16-secMULT1 versus B16 tumors in *Rag2*$^{-/-}$ mice. All experiments show representative examples of ≥3 experiments performed. Tumor volumes ± SE are shown. (A) to (G) were analyzed with two-way ANOVA with Bonferroni multiple comparison tests. $^*P < 0.05$, $^{**}P < 0.01$, $^{***}P < 0.001$ and $^{****}P < 0.0001$.

the clustered regularly interspaced short palindromic repeat (CRISPR)/Cas9 method to disrupt both B6 strain RAE-1 genes, *Raet1d* and *Raet1e*. Peritoneal NK cells from *Raet1d*$^{-/-}$*Raet1e*$^{-/-}$ mice exhibited significant increases in membrane NKG2D expression as well as functional responses (Fig. 4, A to C). Greater differences occurred when the mice were injected with irradiated B16 tumor cells, suggesting that greater NK desensitization and NKG2D down-regulation occurs in the presence of tumors. The increase did not fully account for the effects of secMULT1 (Fig. 4, A and B), suggesting that secMULT1 may also operate by other mechanisms. NK cells in *Raet1*-deficient mice exhibited greater responses to both NKG2D-dependent stimuli (for example, to YAC-1 cells) (Fig. 4B) and NKG2D-independent stimuli (for example, to antibody to NKp46) (Fig. 4C), which is consistent with published reports that persistent stimulation by cells expressing NKG2D ligands results in a global desensitization of NK cells (*17*, *20*). In mice injected with B16-secMULT1 tumor cells, smaller differences were observed, as predicted if secMULT1 blocks NKG2D interactions with RAE-1-expressing cells. Indeed, addition of rMULT1 to cultures of peritoneal wash cells, which contain NK cells and RAE-1^{+} myeloid cells, resulted in increased responses of NK cells to stimulation, when tested 8 to 20 hours later (fig. S11, B and C). These data indicated that interactions of NK cells with RAE-1 molecules on nontumor cells cause NKG2D down-regulation and functional desensitization, and that this may be accentuated in tumor-bearing mice.

Our model further predicts that NKG2D receptor deficiency, or blocking with antibody, should have a similar effect as soluble MULT1. NK cells from NKG2D-deficient (*Klrk1*$^{-/-}$) mice exhibited a modest increase in functional activity (fig. S13A), confirming recent findings (*21*, *22*). A larger effect was evident in NKG2D-deficient NK cells on a *Rag2*$^{-/-}$ background (Fig. 4D). Similarly, intraperitoneal injections of B6 mice with F(ab')$_2$ fragments of blocking NKG2D antibody resulted in enhanced functional responses ex vivo (Fig. 4E). Most remarkably, NKG2D-deficient *Rag2*$^{-/-}$ mice exhibited a strongly enhanced rejection response against B16 and B16-secMULT1 tumors, compared with the responses of *Rag2*$^{-/-}$ mice (Fig. 4, F and G). Furthermore, incorporation of F(ab')$_2$ fragments of blocking NKG2D antibody into B16 tumors that were established in subcutaneous matrigel plugs resulted in partial tumor rejection and augmented responsiveness of NK cells within the residual tumors (fig. S13, B and C). Thus, NKG2D deficiency, or blockade, results in enhanced NK cell responsiveness and tumor rejection. These data strongly support the proposed model (Fig. 3C).

The finding that NK cells persistently stimulated through NKG2D or other receptors are broadly desensitized is consistent with published data (*20*, *23*) and may reflect a defect in mitogen-activated protein kinase (MAPK)/extracellular signal–regulated kinase (ERK) signaling (*23*). Blocking or disabling NKG2D restores killing of B16 cells because NK cells use receptors distinct from NKG2D to target B16 cells. A more complex outcome should pertain with tumor cells that express membrane NKG2D ligands because the NK cells, although more active, will be partly blocked in tumor cell recognition. Tumor cells often express multiple NKG2D ligands, suggesting that therapeutic efficacy may be maximized by blocking only the specific NKG2D ligands expressed by host cells, rather than by blocking NKG2D altogether.

Our results are surprising because they show that soluble NKG2D ligands in vivo stimulate tumor rejection and increase membrane NKG2D, whereas the literature suggests that they should suppress tumor rejection and decrease membrane NKG2D. However, NKG2D down-regulation is frequently not observed in patients with soluble MICA/MICB (*6*–*9*). Moreover, MULT1 and MICA/MICB ligands differ in a key respect: affinity. Soluble MULT1 is a high-affinity (K_d ~ 10 nM) monomeric ligand. Soluble MICA and MICB are low-affinity ligands (K_d ~ 1 μM), which are present in patient sera at concentrations below 1 nM (*4*, *24*), meaning that NKG2D occupancy is predicted to be extremely low. This consideration suggests that systemic effects of soluble MICA and MICB may be indirect, or that the active form of soluble MICA or MICB is actually a multimeric exosome form (*25*, *26*), which can bind and cross-link the receptors despite a low affinity and low concentration. Binding and cross-linking are conditions known to cause modulation of other immune receptors from the cell surface (*27*). B16 cells secreting the low-affinity MICA ligand, when injected intraperitoneally, failed to induce significant NKG2D up-regulation or increased NK functional activity (fig. S14), which is in line with our expectations. The results identify an unexpected mechanism of immune activation and support efforts to evaluate the potential of soluble NKG2D ligands or antibodies that block NKG2D or its ligands for immunotherapy of cancer. Studies suggest that engagement of other NK-activating receptors, such as NKp46, may also lead to NK cell desensitization, suggesting that multiple targets exist for amplifying NK function (*28*).

REFERENCES AND NOTES

1. D. H. Raulet, *Nat. Rev. Immunol.* **3**, 781–790 (2003).
2. D. H. Raulet, S. Gasser, B. G. Gowen, W. Deng, H. Jung, *Annu. Rev. Immunol.* **31**, 413–441 (2013).
3. G. Chitadze, J. Bhat, M. Lettau, O. Janssen, D. Kabelitz, *Scand. J. Immunol.* **78**, 120–129 (2013).
4. V. Groh, J. Wu, C. Yee, T. Spies, *Nature* **419**, 734–738 (2002).
5. H. Song, J. Kim, D. Cosman, I. Choi, *Cell. Immunol.* **239**, 22–30 (2006).
6. H. R. Salih, D. Goehlsdorf, A. Steinle, *Hum. Immunol.* **67**, 188–195 (2006).
7. I. Waldhauer, A. Steinle, *Cancer Res.* **66**, 2520–2526 (2006).
8. K. Wiemann *et al.*, *J. Immunol.* **175**, 720–729 (2005).
9. M. von Lilienfeld-Toal *et al.*, *Cancer Immunol. Immunother.* **59**, 829–839 (2010).
10. N. Guerra *et al.*, *Immunity* **28**, 571–580 (2008).
11. R. A. Eagle *et al.*, *PLOS ONE* **4**, e4503 (2009).
12. M. Xia *et al.*, *Circulation* **124**, 2933–2943 (2011).
13. L. N. Carayannopoulos, O. V. Naidenko, D. H. Fremont, W. M. Yokoyama, *J. Immunol.* **169**, 4079–4083 (2002).
14. T. J. Nice, L. Coscoy, D. H. Raulet, *J. Exp. Med.* **206**, 287–298 (2009).
15. R. Glas *et al.*, *J. Exp. Med.* **191**, 129–138 (2000).
16. A. Diefenbach, E. R. Jensen, A. M. Jamieson, D. H. Raulet, *Nature* **413**, 165–171 (2001).
17. D. E. Oppenheim *et al.*, *Nat. Immunol.* **6**, 928–937 (2005).
18. C. A. Crane *et al.*, *Proc. Natl. Acad. Sci. U.S.A.* **111**, 12823–12828 (2014).
19. N. Nausch, I. E. Galani, E. Schlecker, A. Cerwenka, *Blood* **112**, 4080–4089 (2008).
20. J. D. Coudert, L. Scarpellino, F. Gros, E. Vivier, W. Held, *Blood* **111**, 3571–3578 (2008).
21. B. Zafirova *et al.*, *Immunity* **31**, 270–282 (2009).
22. S. Sheppard *et al.*, *Blood* **121**, 5025–5033 (2013).
23. M. Ardolino *et al.*, *J. Clin. Invest.* **124**, 4781–4794 (2014).
24. A. Märten, M. von Lilienfeld-Toal, M. W. Büchler, J. Schmidt, *Int. J. Cancer* **119**, 2359–2365 (2006).
25. A. Clayton *et al.*, *J. Immunol.* **180**, 7249–7258 (2008).
26. O. Ashiru *et al.*, *Cancer Res.* **70**, 481–489 (2010).
27. R. B. Taylor, W. P. Duffus, M. C. Raff, S. de Petris, *Nat. New Biol.* **233**, 225–229 (1971).
28. E. Narni-Mancinelli *et al.*, *Science* **335**, 344–348 (2012).

ACKNOWLEDGMENTS

We thank H. Nolla and A. Valeros for help with cell sorting; C. Kang for targeting eggs for creating the *Raet1* knockout mice; Q. Yan for assistance with Biacore assays; and T. Trevino, L. Bai, S. Li for technical assistance. We thank Raulet Lab members and R. Vance for useful discussion and comments on the manuscript. The data presented in this manuscript are tabulated in the main paper and in the supplementary materials. D.H.R. is an inventor on a patent (U.S. 6821522) filed by University of California, Berkeley describing the use of soluble ligands for immunotherapy of cancer. W.D. was supported by a Cancer Research Institute postdoctoral fellowship. B.G.G. was supported by a National Science Foundation Graduate Research Fellowship and the Hirth Chair Graduate Fellowship of University of California, Berkeley. L.W. and A.I. were supported by Leukemia and Lymphoma Society Fellowships, and S.L. was supported by a NIH–Initiative for Maximizing Student Development grant. This work was supported by NIH grant R01 CA093678 to D.H.R.

SUPPLEMENTARY MATERIALS

www.sciencemag.org/content/348/6230/136/suppl/DC1
Materials and Methods
Supplementary Text
Fig. S1 to S14
Table S1
References (*29*–*32*)

17 July 2014; accepted 30 January 2015
Published online 5 March 2015;
10.1126/science.1258867

A shed NKG2D ligand that promotes natural killer cell activation and tumor rejection

Weiwen Deng *et al.*

Science **348**, 136 (2015);
DOI: 10.1126/science.1258867

www.sciencemag.org/cgi/content/full/science.1258867/DC1

Supplementary Material for

A shed NKG2D ligand that promotes natural killer cell activation and tumor rejection

Weiwen Deng, Benjamin G. Gowen, Li Zhang, Lin Wang, Stephanie Lau, Alexandre Iannello, Jianfeng Xu, Tihana L. Rovis, Na Xiong, David H. Raulet*

*Corresponding author. E-mail: raulet@berkeley.edu

Published 5 March 2015 on *Science* Express
DOI: 10.1126/science.1258867

This PDF file includes:

Materials and Methods

Cells, antibodies and reagents

Cell culture was performed at 37°C in humidified atmosphere containing 5% CO_2. Fibroblasts and B16 cells were cultured in complete DMEM, consisting of DMEM (Invitrogen), 10% fetal calf serum (Omega Scientific), 100 U/ml penicillin (Invitrogen), 100 µg/ml streptomycin (Invitrogen), 0.2 mg/ml glutamine (Sigma-Aldrich), 10 µg/ml gentamycin sulfate (Lonza), 20 mM HEPES (Thermo Fisher Scientific), and 50 µM 2-mercaptoethanol (EMD Biosciences). RMA and YAC-1 cells were cultured in similarly supplemented RPMI medium.

Antibodies against NK1.1 (PK136), CD3ε (145-2C11), CD45.2 (104), IFN-γ (XMG1.2), CD107a (1D4B), NKG2D (MI6), NKp46 (29A1.4), CD11b (M1/70) and F4/80 (BM8) were purchased from eBioscience. Monoclonal HA antibody (clone 16B2) was from Covance. Anti–panRAE-1 (clone 186107), anti-MULT1 antibody (clone 237104, clone 1D6), RAE1-Fc and recombinant MULT1 were from R&D Systems. NK1.1 (PK136) and CD8 (2.43) antibodies for in vivo depletions were prepared in the laboratory or purchased from BioXCell.

Mice and *in vivo* procedures

All mice were bred at the University of California, Berkeley, in compliance with institutional guidelines. C57BL/6J (hereafter called B6), B6-*Eμ-Myc* transgenic and B6-*Rag2*-/- mice were purchased from the Jackson Laboratory. The B6-*Klrk1*$^{-/-}$ (NKG2D KO) strain (*10*) is available at the Jackson Laboratory Repository (JAX Stock No. 022733). B6-*Rag2*$^{-/-}$ and B6-*Klrk1*$^{-/-}$ mice were intercrossed two generations to generate B6-*Rag2*$^{-/-}$*Klrk1*$^{-/-}$ mice (*29*). NKG2D-deficient mice were screened for the *Klrk1* deletion by genomic PCR. All mice were used between 6 and 12 weeks of age.

Conventional subcutaneous tumors were generated by injecting cells subcutaneously in 100 µl PBS in the right flank. Tumor growth was monitored by measuring the tumor size twice

weekly with a metric caliper. For short-term experiments, tumor cells were injected S.C. in the right flank after resuspending in 100 μl matrigel, matrix growth factor reduced (BD Bioscience), and, where indicated, adding recombinant proteins. In this case, tumor size was determined as the weight of the tumor plug or tumor cell numbers (after dissociation, described in ***In vivo and ex vivo* analyses**). The tumor experiments typically included 3-15 (usually 4-6) mice per group.

When indicated, NK cells and CD8+ T cells were depleted from mice in vivo by intraperitoneal injection of 200 μg NK1.1 (PK136), CD8 (2.43) or control IgG antibody at days -1, 1, 8, 15, and 22. Depletions were confirmed by flow cytometric analysis of spleen cells 3 weeks after tumor challenge using non-competing antibodies.

Generation of *Raet1* KO mice

Raet1 mutant mice were generated using the CRISPR/Cas9 system. We chose a shared Cas9 target site present in the second coding exon of the highly related *Raet1d* and *Raet1e* genes. *Cas9* mRNA and the *Raet1* sgRNA were *in vitro* transcribed and injected into single-cell embryos as described (*30*). F_0 mice carrying frame-shift mutations in both *Raet1d* and *Raet1e* genes were identified by PCR and were back-crossed to C57BL/6 mice, and the resulting *Raet1* heterozygous F_1 mice were intercrossed to produce the mice used in this study. *Raet1*$^{-/-}$ mice from one founder line, in which both genes contained frame-shift mutations, were used in this study. *Raet1* genomic target sequence with protospacer-adjacent motif (PAM, underlined): 5'-TAGGTGCAACTTGACCATCAAGG-3'. Oligonucleotides used to clone the *Raet1* sgRNA:

Fwd: 5'-CACCGGTAGGTGCAACTTGACCATCA-3',

Rev: 5'-AAACTGATGGTCAAGTTGCACCTACC-3'.

The underlined GG dinucleotide, which is not present in the genomic target sequences, was added to the 5' end of the sgRNA sequence to allow for better transcription from the T7 promoter.

Constructs and transduction of cells

Segments encoding epitope tagged full length MULT1 (a mutant version (KR) in which the six lysine residues in the cytoplasmic tail were mutated to arginines in order to optimize cell surface expression (*14*)), secMULT1 (amino acids 1-211), and secMICA (amino acids 1-307) were cloned into the pMSCV2.2-IRES-GFP retroviral vector. Retroviral supernatants were generated by cotransfecting 293T cells with plasmids encoding VSV gag/pol and env and pMSCV retroviral constructs, using Lipofectamine 2000 (Invitrogen). Culture supernatants collected 48 h after transfection were added directly to actively proliferating cells, and transduced cells were sorted based on GFP expression. A segment encoding secMULT1 (no tag) was also cloned into a Tet-inducible lentiviral vector pFG12-TRE-UbC-rtTA-Thy1.1, and transduced cells were selected based on Thy1.1 expression. For induction in vitro, cells were cultured in 100 ng/ml doxycycline (Sigma-Aldrich) in complete DMEM medium. For induction in vivo, the drinking water was supplemented with 0.2 mg/ml doxycycline in 0.5% sucrose solution, which was kept in light-protected bottles and refreshed every week.

Immunoprecipitation and Immunoblot Analysis

Transduced fibroblasts were cultured in serum-containing medium (5%) for 48 hours and switched to serum-free medium for 24 hours. Supernatants were collected and concentrated with 10 kDa Amicon Ultra-15 Centrifugal filter Units (Millipore). Protease inhibitor mixture tablets (Roche, Basel, Switzerland) were added to the supernatants. Immunoprecipitation, PNGaseF

treatment and immunoblot analysis of supernatants and cell lysates were performed as previously described (*31*).

MULT1 sandwich ELISA

In brief, plates were coated with 2 μg/ml of MULT1 capture antibody (clone 237104, R&D) overnight at 4°C. After blocking with 2% BSA-PBST (0.05% Tween 20 in PBS), plates were washed with PBST. Samples, or recombinant MULT1 (R&D) (which served as a standard), were diluted in PBST and incubated overnight at 4°C. After washing, biotinylated MULT1 detecting antibody (clone 1D6) was added at a concentration of 1 μg/ml. After incubation and washing, HRP-conjugated streptavidin (BD Pharmingen, diluted 1/2000) was applied. Plates were washed extensively before adding the peroxidase substrate TMB (Sigma). HRP activity was stopped by addition of H_2SO_4, and absorbance was measured at 450 nm. Male *Apoe*-/- mice were fed on a high fat diet for two months, starting at the age of six weeks, before their sera were collected, as previously described (*12*).

Purification of MULT1 protein and MI6 F(ab')$_2$

Shed MULT1 and secMULT1 were purified from concentrated supernatants of fibroblasts transduced with HA-MULT1 (KR) and HA-secMULT1, by HA immunoprecipitation followed by elution with HA peptide (Sigma-Aldrich). The HA peptide was removed with 10 kD Amicon Ultra-15 Centrifugal filter units.

MI6 F(ab')$_2$ fragments were prepared using immobilized pepsin (Pierce) according to the manufacturer's instructions. After purification of F(ab')$_2$ fragments with 50 kD Amicon Ultra-15 Centrifugal filter units, no Fc fragments or intact antibody were detected by SDS-PAGE. Rat IgG F(ab')$_2$ (Jackson Immunoresearch) was used as a control.

Surface plasmon resonance (SPR) assay

All experiments were performed on a BIAcore 2000 (Biacore) at 25°C using HBS-P (Fisher Scientific) as flow buffer. Biotin-NKG2D or biotin-CD19 was affixed to SA sensor chip (GE) with the desired level of Rmax (300-400 RU). ShedMULT1 and secMULT1 (1, 2, 5,10, 20 nM) were sequentially analyzed for binding to SPR flow cells derivatized with biotin-anti-CD19 (negative control) or biotin-NKG2D. Flow rates were 10 μl/min and regeneration was performed for 30s with 100 mM NaOH. Steady-state experiments were performed in triplicate over two separate surfaces. Raw data were analyzed and graphed using BIAeval 3.1 (BIAcore) and Prism Software.

***In vivo and ex vivo* analyses**

In preparation for ex vivo analyses, 5 x 10^6 irradiated tumor cells (120 Gy) were injected intraperitoneally as described (*15*). Peritoneal cells were collected after 3 days and were examined by flow cytometry or used to sort NK cells and prepare RNA for RT-qPCR analysis. Peritoneal wash cells were pooled for cytotoxicity and IFN-γ assays.

Fresh tumor tissues or matrigel plugs were excised from mice, weighed, minced, and dissociated using the gentleMACS Dissociator (Miltenyi Biotec). Dissociated tumor samples were further digested in RPMI containing 200 μg/ml Collagenase IV (Roche) and 20 μg/ml DNase I (Sigma-Aldrich) at 37°C for 30 min. After filtering through a 40 μm nylon mesh, single cell suspensions were counted and used for experiments.

Antibody staining and flow cytometry analysis

Dead cells were excluded by staining with Live-Dead fixable dead cell stain kit (Molecular Probes, Grand Island, NY) following manufacturer's instructions. Before staining, cells were preincubated for 20 min with 2.4G2 hybridoma supernatant to block FcrRII/III receptors. Cells

were stained with the specified antibodies in 50 μl of PBS supplemented with 2% FCS (FACS buffer). Intracellular staining was performed after surface staining with the Cytofix/Cytoperm kit (BD Bioscience) according to manufacturer's instructions. Multicolor flow cytometry was performed on a cytometer (LSRII; BD), and data were analyzed with FlowJo software (Tree Star, Inc.).

Cytotoxicity and IFNγ assays

NK cell cytotoxicity was determined with a standard 4-h ^{51}Cr-release assay, with pools of cells from five mice, tested in quadruplicate (*29*). The spontaneous release was, in all cases, <20% of the maximum release. The percentage of specific ^{51}Cr release was calculated according to the following formula: % specific lysis = 100 × (experimental release − spontaneous release)/(detergent release − spontaneous release). In some experiments, LIVE/DEAD fixable stain kits (Invitrogen) were used to measure the killing of target cells (GFP^+) (*32*). NK cells and the target cells were incubated for 2 h and the total cells were stained with LIVE/DEAD fluorescent dye to detect dead cells. The percentages of violet cells (dead cells) in the GFP^+ population were used to calculate the percentages of specific lysis according to the following formula: % specific lysis = 100 x (%dead cells in experimental sample - %dead cells in spontaneous control sample)/ (100% - %dead cells in spontaneous control sample).

For assaying IFNγ producing cells, $2x10^5$ – $1x10^6$ cells were stimulated in flat-bottomed, high protein-binding plates (Thermo Fisher Scientific, Waltham, MA) for 4h in the presence of 1 μg/ml GolgiPlug (BD) and 1000 U/ml recombinant human IL-2 (National Cancer Institute), before staining the cells for intracellular IFNγ. For some of experiments, CD107a staining was also assayed. For those experiments, an additional 1 μg/ml GolgiStop (BD) and CD107a antibody were added to the wells before stimulation. As indicated, the wells were coated with 5 μg/ml NKG2D, 50 μg/ml NKRP1C, or 5 μg/ml NKp46 antibodies. In other cases the wells

contained an equal number of tumor target cells. Between 3 and 12 (usually 4-5) replicate samples per group were compared.

Quantitative RT-PCR

Total RNA was isolated using Trizol LS (Invitrogen), followed by digestion of contaminating DNA using DNA-free (Ambion) according to the manufacturer's protocol. RNA was reverse transcribed to cDNA using iScript reverse transcription system (Bio-Rad Laboratories) according to the manufacturer's instructions. Quantitative real-time PCR was performed on a CFX96 thermocycler (Bio-Rad Laboratories) using SSO-Fast EvaGreen Supermix (Bio-Rad Laboratories). 18S rRNA and RPL19 were used as references. The primers used for qRCR analyses are listed in Table S1.

Gel filtration FPLC

Concentrated supernatants of Fibro-MULT1 and RMA-secMULT1 were fractionated by Gel filtration chromatography with a Superdex 200 column on an FPLC system. Pools correspond to >85 kD (1-10), ~65-85 kD (11-20), ~50-65 kD (21-30), ~35-50 kD (31-40), ~20-35 kD (41-50), <20 kD (51-60).

Statistical analysis

Statistical comparisons were performed with the Prism software (GraphPad Software). P-values were determined as follows:

2 way ANOVA with Bonferroni multiple comparison tests: Figures 1B-E, 2A-D, 2F, 3B, 4A-G, Figures S4A, S5, S8A, S8B, S11A-C and S13A, S13C.

One-way ANOVA Kruskal-Wallis test with Dunn's multiple comparisons: Figure 3A, Figure S7.

One-way ANOVA, after Kolmoogorv-Smirnov normality test, with Bonferroni's multiple comparison tests: Figures S14A, S14B.

Mann-Whitney tests: Figure 1A, Figure 2E and Figures S12 and S13B.

Differences between groups were considered significant for P-values <0.05. $*P < 0.05$, $**P < 0.01$, $***P < 0.001$ and $****P < 0.0001$.

Table S1. List of forward and reverse primers used in Q-RT-PCR and the amplicon size for each target

Target	Forward (F) and reverse (R) primers (5'-3')	Amplicon size
Klrk1	F: ACAGGATCTCCCTTCTCTGCT	75bp
	R: AAGTATCCCACTTTGCTGGCT	
Rn 18s	F: GTCTGTGATGCCCTTAGATG	177bp
	R: AGCTTATGACCCGCACTTAC	
Rpl19	F: AGCCTGTGACTGTCCATTCC	98bp
	R: GGCAGTACCCTTCCTCTTCC	
Il1b	F: CAACCAACAAGTGATATTCTCCATG	155bp
	R: GATCCACACTCTCCAGCTGCA	
Il6	F: CTGCAAGAGACTTCCATCCAGTT	70bp
	R: GAAGTAGGGAAGGCCGTGG	

Figure S1

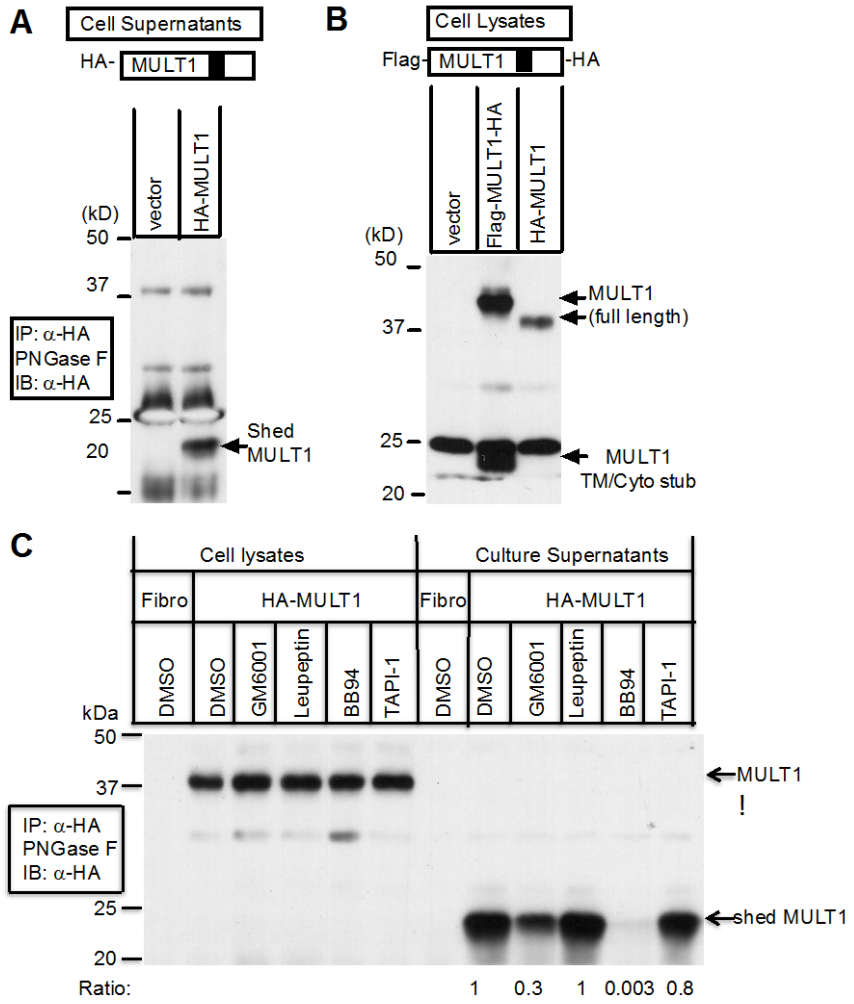

Fig. S1. MULT1 is shed from cell surface. (A) The extracellular domain MULT1 fragment ("shedMULT1") detected in supernatants of fibroblasts transduced with N-terminally HA-tagged MULT1 (HA-MULT1), after HA immunoprecipitation, treatment with PNGaseF to remove N-glycans, and blotting with HA antibody. (B) C-terminal MULT1 "stub" and full length MULT1 detected in lysates of fibroblasts transduced with C-terminally tagged MULT1 (MULT1-HA) (middle lane) after HA immunoprecipitation, treatment with PNGaseF, and blotting with HA antibody. The band at 25 kD was a background band. The relative intensity of the full length and stub bands suggests that most MULT1 is cleaved in these cells, and the fragment sizes suggest that the protein is cleaved near the plasma membrane. (C) Shedding of MULT1 is inhibited by Matrix metalloproteinase (MMP) inhibitors. HA-MULT1 transduced fibroblasts were treated with DMSO, the broad-spectrum inhibitor of MMPs and other metalloproteinases BB-94 (5 μM), the broad spectrum MMP inhibitor GM6001 (10 μM), a cysteine/serine/threonine protease inhibitor leupeptin (10 μM), or an ADAM17 inhibitor TAPI-1 (10 μM) for 24 hours in serum-free medium. Cell lysates and concentrated supernatants were subjected to HA immunoprecipitation and PNGase F treatment followed by HA immunoblotting. All experiments were performed at least twice.

Figure S2

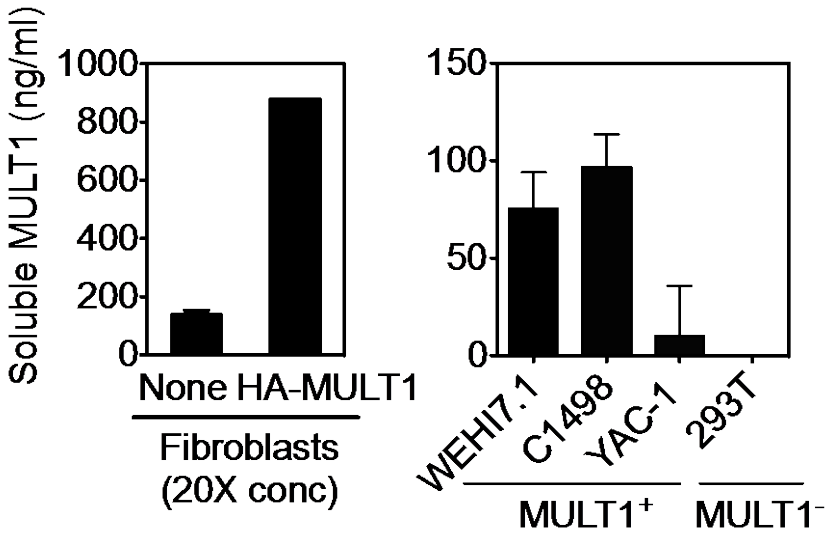

Fig. S2. MULT1 is released from cell lines that naturally or ectopically express MULT1. ELISA detection of soluble MULT1 in 20x concentrated culture supernatants of transduced fibroblasts, or the indicated unconcentrated supernatants of untransduced cell lines that do or don't express MULT1 (as indicated). This experiment was performed twice with similar results.

Figure S3

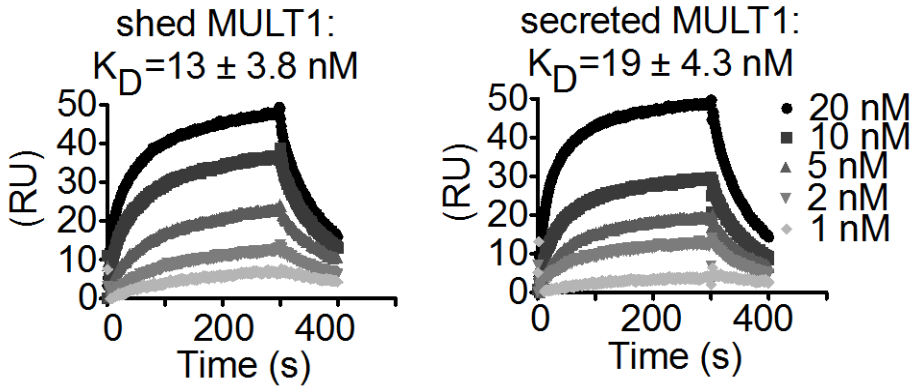

Fig. S3. shedMULT1 and secMULT1 bind to NKG2D with high affinity. Surface plasmon resonance analysis of binding of shed MULT1 and secreted MULT1 (secMULT1) to chip-bound recombinant NKG2D. ShedMULT1 and secMULT1 (1, 2, 5,10, 20 nM) were sequentially analyzed for binding to SPR flow cells derivatized with biotin-anti-CD19 (negative control) or biotin-NKG2D. This experiment was performed three times. Average of K_D ±SE was shown.

Figure S4

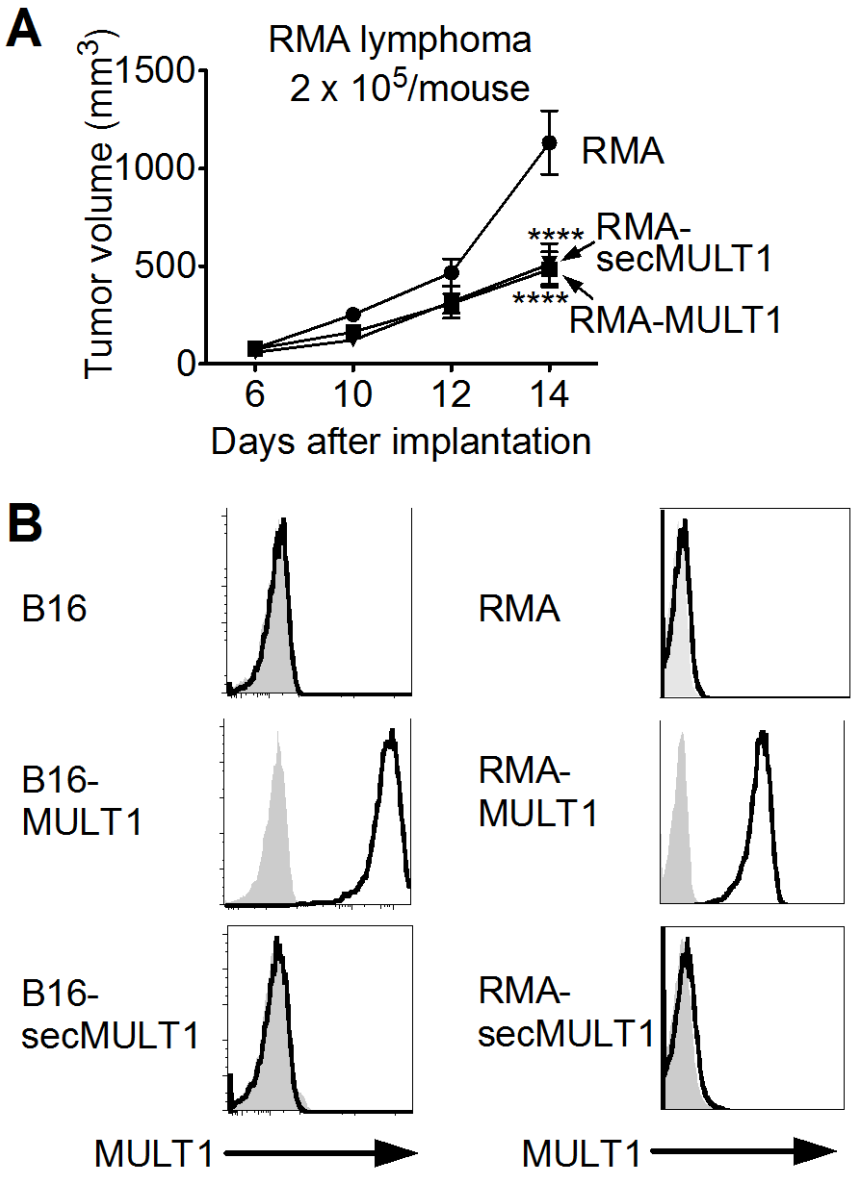

Fig. S4. RMA tumor cells expressing secMULT1 are rejected. (A) Comparison of subcutaneously transferred RMA lymphoma tumor cells transduced with secMULT1, full length MULT1 or empty vector, in WT B6 (syngeneic) mice (n=4). Analyzed by 2-way ANOVA with Bonferroni multiple comparison tests. ****$P < 0.0001$. (B) RMA cells or B16 cells (before injection) were stained with MULT1 Abs. Grey shows isotype control staining. All experiments were performed at least three times.

Figure S5

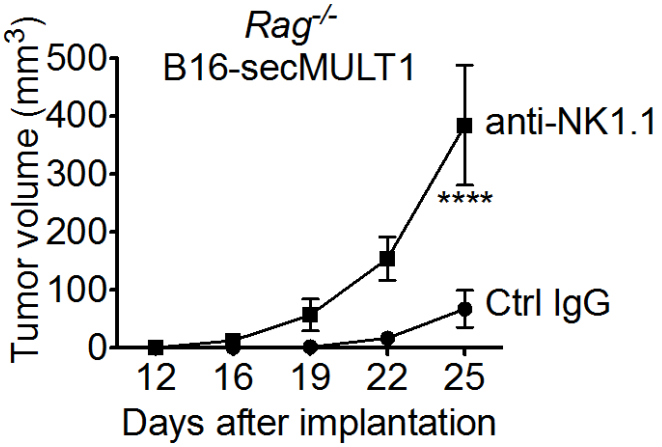

Fig. S5. NK cells participate in the rejection of B16-secMULT1 cells. Subcutaneous growth of B16-secMULT1 tumors in B6-*Rag1*$^{-/-}$ mice (1 x 10^4 cells were inoculated, n=5) treated with control IgG or NK1.1 antibody (PK136) to deplete NK cells. This experiment was performed three times. Analyzed by 2-way ANOVA with Bonferroni multiple comparison tests. ****$P < 0.0001$.

Figure S6

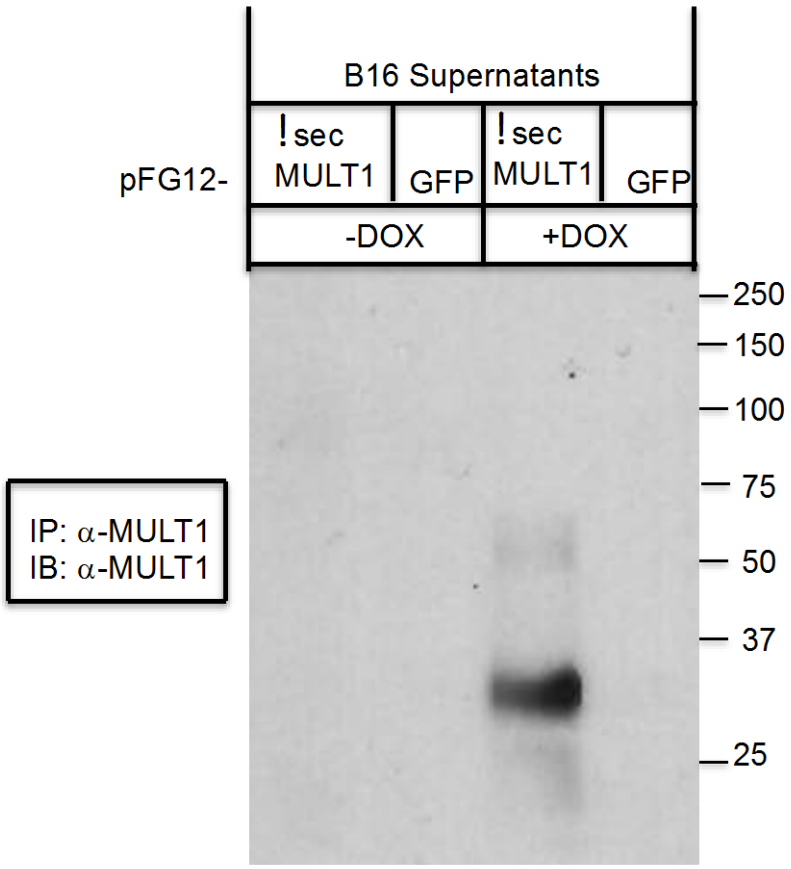

Fig. S6. Inducible expression of secMULT1 in B16 tumor cells. B16-pFG12-secMULT1 or B16-pFG12-GFP cells were cultured with or without 100 ng/ml doxycycline (Sigma-Aldrich) in complete DMEM medium for 4 days, at which time culture supernatants were concentrated and subjected to MULT1 immunoprecipitation, immunoblotting and gel analysis. This experiment was performed twice with similar results.

Figure S7

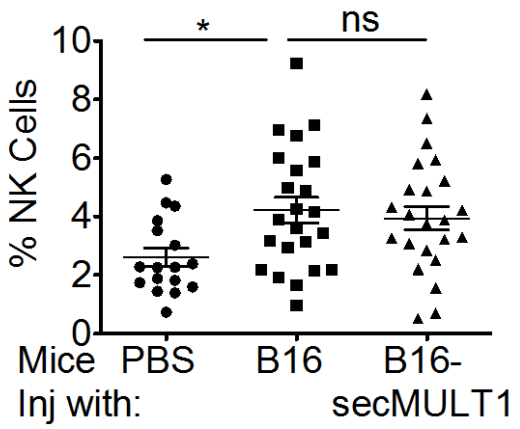

Fig. S7. Increased NK cell percentages among peritoneal wash cells in mice injected i.p. with irradiated B16 or B16-secMULT1 tumor cells. B6 mice were injected i.p. with 5 x 10^6 irradiated (120Gy) B16 or B16-secMULT1 cells, or with PBS. Peritoneal wash cells were recovered three days later. Percentages of NK ($NK1.1^+CD3^-$) cells were determined by flow cytometry. N=17-24 mice per group, which represents combined data from 7 experiments. Analyzed by One-way ANOVA Kruskal-Wallis test with Dunn's multiple comparisons, $*P < 0.05$, ns indicates $P > 0.05$.

Figure S8

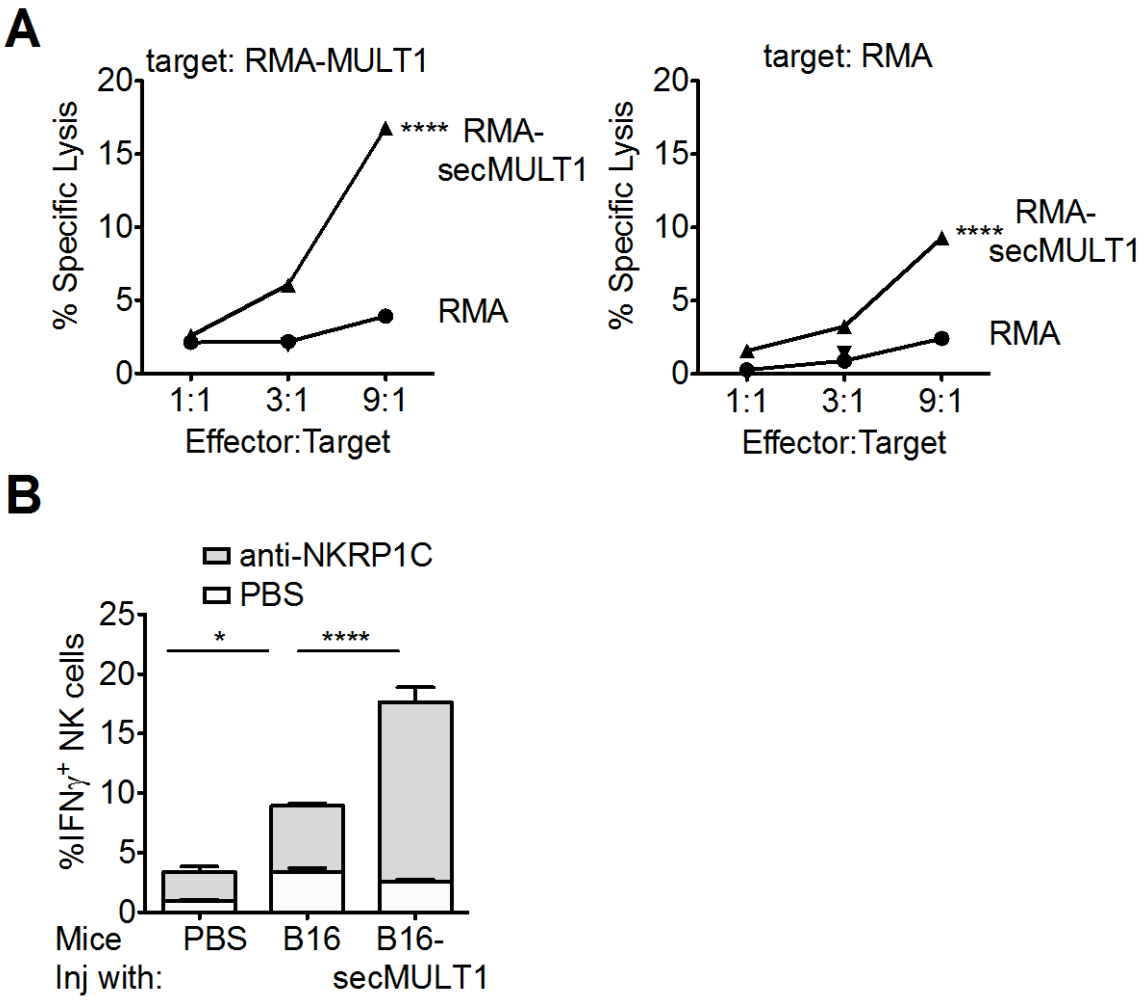

Fig. S8. Exposure to secMULT1 expressing RMA or B16 cells induces NK activity. (A) B6 mice were injected i.p. with 2 x 10^6 irradiated (120 Gy) RMA or RMA-secMULT1 cells. 3 days later, peritoneal wash cells were harvested and tested for killing of RMA-MULT1 (left) or RMA (right) target cells in vitro. For both target cell types, RMA-secMULT1-induced killing was significantly higher than RMA-induced killing. (B) B6 mice were injected i.p. with 5 x 10^6 irradiated (120Gy) B16 or B16-secMULT1 cells, or with PBS. Peritoneal wash cells were recovered three days later and stimulated with immobilized NKRP1C for 4 hours and tested for intracellular IFNγ, control responses to PBS are depicted by white segments of the bars. All experiments were performed twice with similar results. Analyzed by 2-way ANOVA with Bonferroni multiple comparison tests. * $P < 0.05$, **** $P < 0.0001$.

Figure S9

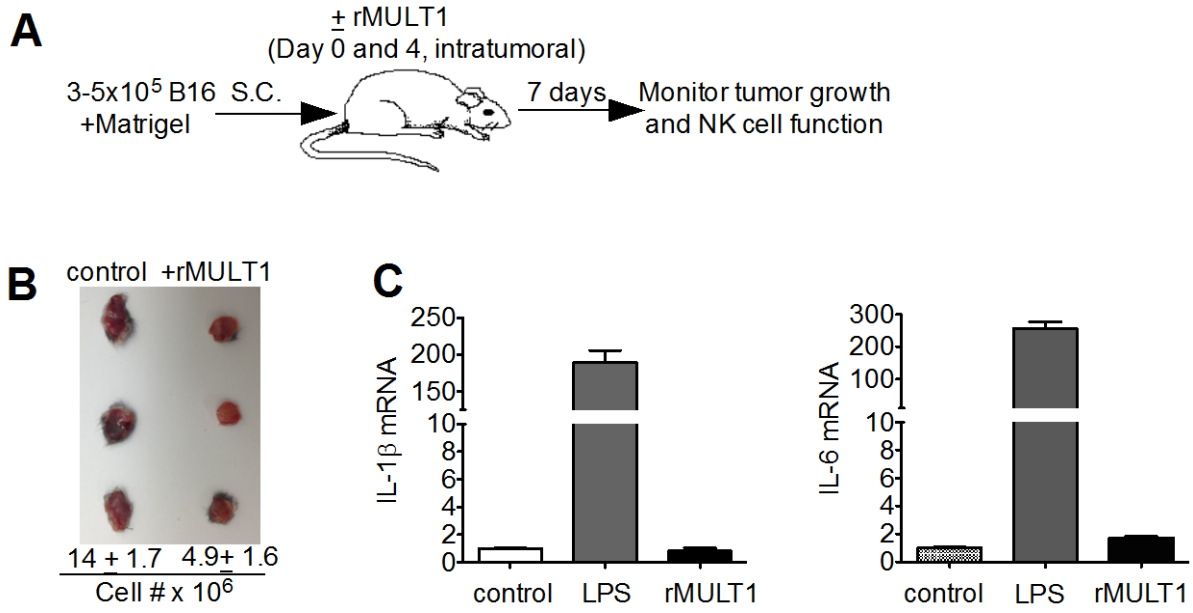

Fig. S9. Recombinant MULT1 causes tumor rejection. (A, B) Subcutaneous tumors were established with 3-5 x 10^5 B16 cells in 100 μl matrigel. The tumor cells in one group were mixed with 1 μg of recombinant MULT1 (rMULT1). After 4 days, an additional 1 μg of rMULT1 was injected into each matrigel/tumor for that group. Tumors in the control group received PBS. On day 7, tumors were extracted for experiments. Panel B was one of four repetitions of the experiment presented in **Fig. 2E.** (C) rMULT1 failed to stimulate peritoneal wash cells to produce IL-1β and IL-6 in a 4 h stimulation period, indicating the absence of endotoxin or other PAMPs that stimulate macrophages. Peritoneal wash cells were collected from B6 mice and cultured with PBS, 20 ng/ml LPS or 10 μg/ml recMULT1 for 4 hours. Cells were harvested and used to prepared RNA for RT-qPCR analysis. Panel C was performed twice with similar results.

Figure S10

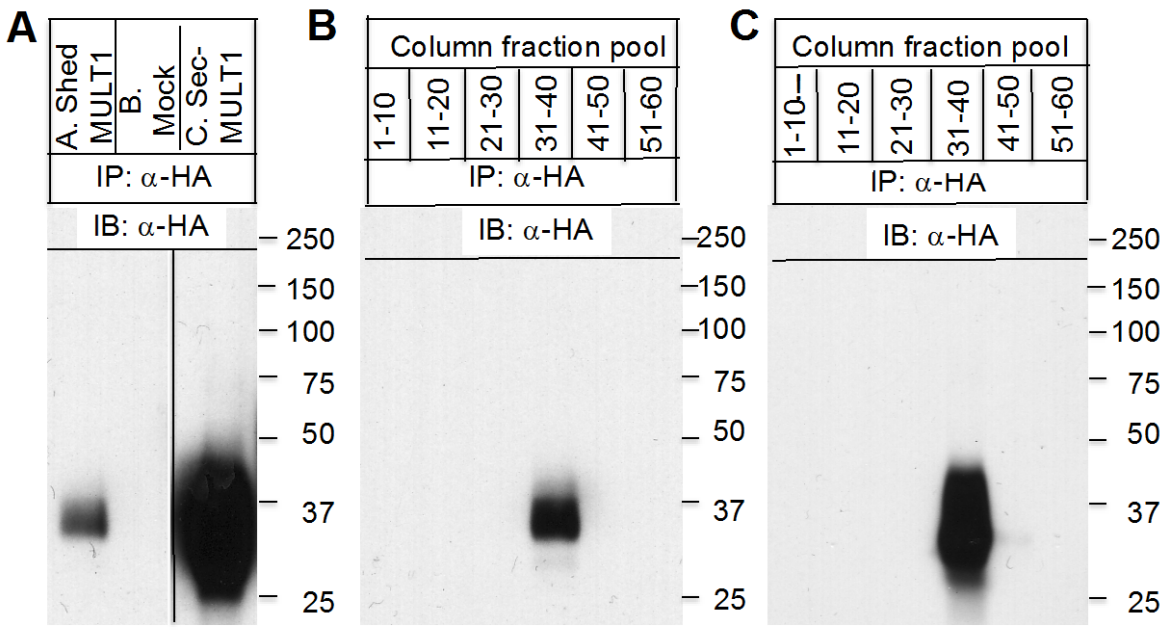

Fig. S10. Soluble MULT1 is monomeric. (A) Shed MULT1 and secMULT1 exhibit similar apparent molecular weights (~35 kD), based on Western blots of HA immunoprecipitates of samples from fibroblasts transduced with full length MULT1 and secMULT1. Lanes from the same gel were spliced together for simplicity. (B, C) Shed MULT1 and secMULT1 are monomeric. Concentrated shed MULT1 (B) or secMULT1 (C) were fractionated by S200 gel filtration FPLC, and fraction pools were immunoprecipitated and blotted with HA Abs. Pools correspond to >85 kD (1-10), ~65-85 kD (11-20), ~50-65 kD (21-30), ~35-50 kD (31-40), ~20-35 kD (41-50), <20 kD (51-60). All experiments were performed at least twice.

Figure S11

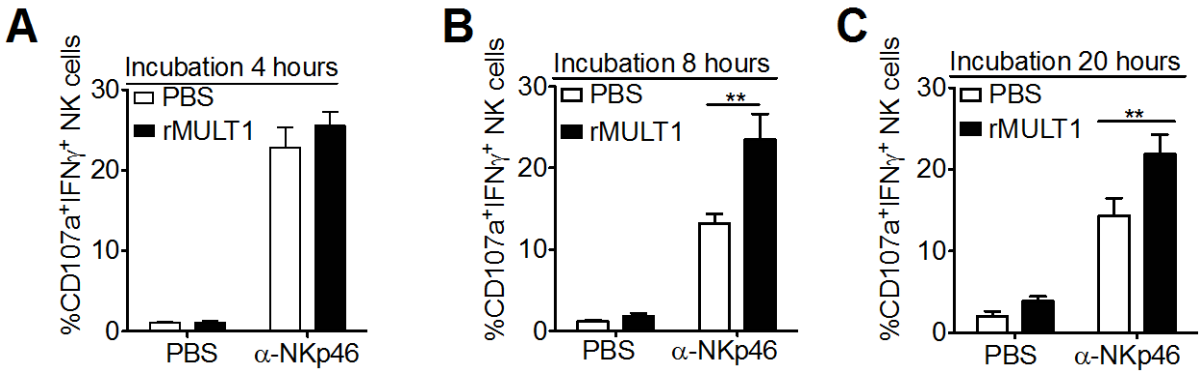

Fig. S11. Sustained exposure of peritoneal NK cells to rMULT1 in vitro amplifies NK functions. Peritoneal wash cells, which include NK cells and RAE-1+ myeloid cells, among other cell types, were incubated for 4, 8 or 20 hours with the addition of 10 μg/ml rMULT1 or PBS to the cultures. For the 4 hr timepoint, cells were incubated with rMULT1 during the stimulation assay. For the 8 hr timepoint, cells were incubated with rMULT1 for 4 hrs before addition to stimulation wells for an additional 4 hrs. For the 20 hr timepoint, cells were incubated with rMULT1 for 16 hrs before addition to stimulation wells for an additional 4 hrs. Note that NK cell activity diminishes after prolonged in vitro culture, and therefore the control responses for different time points cannot be directly compared. All experiments were performed at least twice. Analyzed by 2-way ANOVA with Bonferroni multiple comparison tests. $^{**}P < 0.01$.

Figure S12

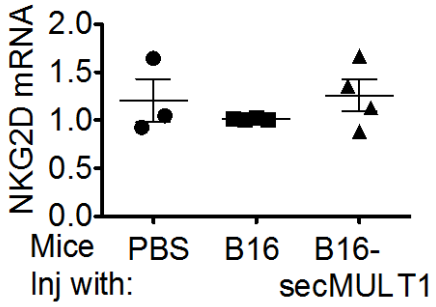

Fig. S12. No increase in NKG2D mRNA after exposure to secMULT1 in intraperitoneal tumors. Mice were injected i.p. with PBS, 5 x 10^6 irradiated B16 or B16-MULT1 cells, and peritoneal wash cells were harvested 3 days later and used to sort NK cells and prepare RNA for RT-qPCR analysis. RNA from 4 independent experiments was collected for RT-qPCR. Each point represents a different RNA sample.

Figure S13

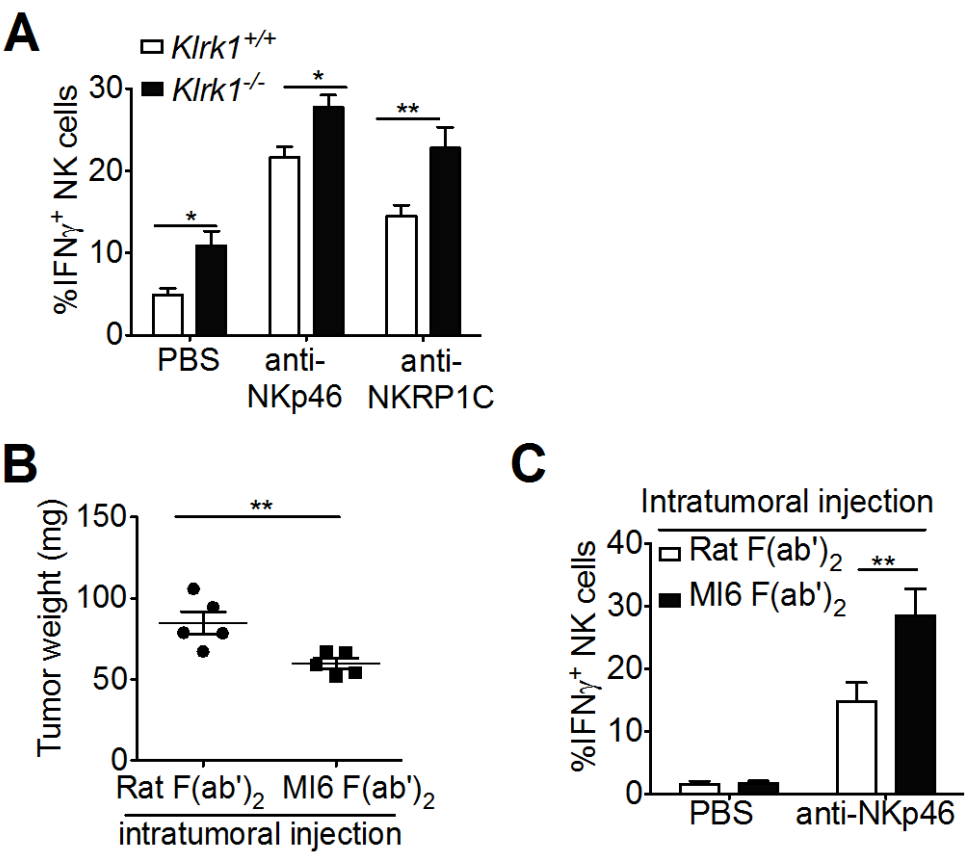

Fig. S13. Blockade or absence of NKG2D result in increased NK functional activity. (A) Splenic NK cells from B6 WT and NKG2D-deficient mice were stimulated *ex vivo* with immobilized NKp46 or NKRP1C Abs, and the IFN-γ responses of gated NK cells were determined. (B) Subcutaneous tumors were established with 5 x 10^5 B16 cells in 100 μl matrigel, to which was added either 10 μg of MI6 $F(ab')_2$ or $F(ab')_2$ of rat IgG. After 4 days, an additional 10 μg of $F(ab')_2$ (or control $F(ab')_2$) was injected into the matrigel/tumors. On day 7, tumors were extracted and weighed (B). The tumors were then dissociated, the cells within the tumor were stimulated with immobilized NKp46 Abs, and the IFNγ responses of gated NK cells were determined (C). All experiments were performed three times. Panels A and C were analyzed by 2-way ANOVA with Bonferroni multiple comparison tests, panel B was analyzed by Mann-Whitney test. $*P < 0.05$, $**P < 0.01$.

Figure S14

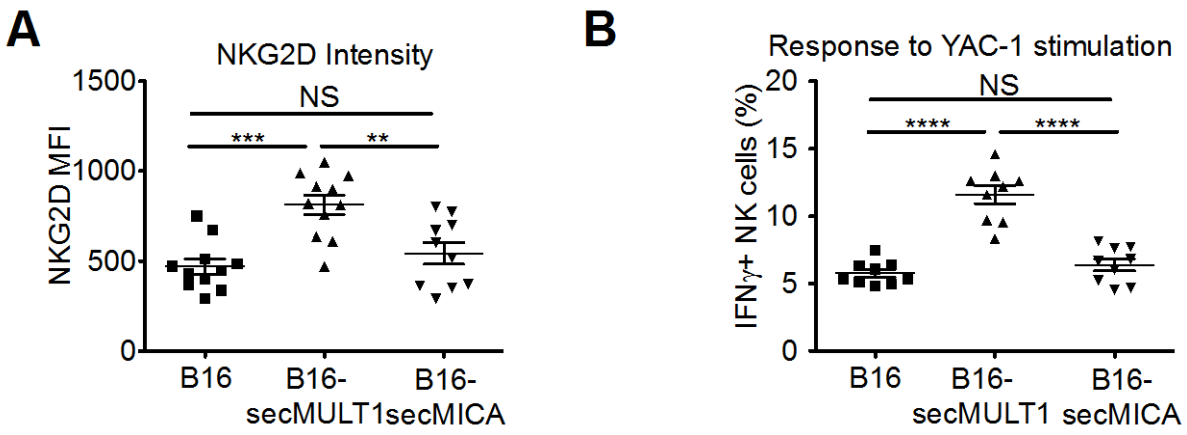

Fig. S14. secMICA fails to restore NK responses. B6 mice received i.p. injections of 5 x 10^6 irradiated B16 cells, B16-secMULT1 cells or B16-secMICA cells. Three days later peritoneal wash cells were harvested and either stained with NKG2D antibody (A) or stimulated in vitro with YAC-1 tumor cells before performing staining for intracellular IFN-γ (B). The secMICA fragment corresponded to amino acids 1-307 of MICA. All experiments include combined data from 3 experiments. Analyzed by One-way ANOVA, after Kolmogorv-Smirnov normality test, with Bonferroni's multiple comparison tests. $^{**}P < 0.01$, $^{***}P < 0.001$ and $^{****}P < 0.0001$.

Author Contributions:

WD designed, executed and analyzed the experiments. BG led the effort to generate the *Raet1* knockout mice. LZ, LW, SL, AI, JX assisted with experiments. NX prepared the sera samples from *Apoe*$^{-/-}$ mice. TR prepared the 1D6 MULT1 antibody. DHR conceived of the study, and with WD, designed and interpreted the experiments. The manuscript was prepared by WD and DHR. All authors critically read the manuscript.

References and Notes

1. D. H. Raulet, Roles of the NKG2D immunoreceptor and its ligands. *Nat. Rev. Immunol.* **3**, 781–790 (2003). Medline doi:10.1038/nri1199

2. D. H. Raulet, S. Gasser, B. G. Gowen, W. Deng, H. Jung, Regulation of ligands for the NKG2D activating receptor. *Annu. Rev. Immunol.* **31**, 413–441 (2013). Medline doi:10.1146/annurev-immunol-032712-095951

3. G. Chitadze, J. Bhat, M. Lettau, O. Janssen, D. Kabelitz, Generation of soluble NKG2D ligands: Proteolytic cleavage, exosome secretion and functional implications. *Scand. J. Immunol.* **78**, 120–129 (2013). Medline doi:10.1111/sji.12072

4. V. Groh, J. Wu, C. Yee, T. Spies, Tumour-derived soluble MIC ligands impair expression of NKG2D and T-cell activation. *Nature* **419**, 734–738 (2002). Medline doi:10.1038/nature01112

5. H. Song, J. Kim, D. Cosman, I. Choi, Soluble ULBP suppresses natural killer cell activity via down-regulating NKG2D expression. *Cell. Immunol.* **239**, 22–30 (2006). Medline doi:10.1016/j.cellimm.2006.03.002

6. H. R. Salih, D. Goehlsdorf, A. Steinle, Release of MICB molecules by tumor cells: Mechanism and soluble MICB in sera of cancer patients. *Hum. Immunol.* **67**, 188–195 (2006). Medline doi:10.1016/j.humimm.2006.02.008

7. I. Waldhauer, A. Steinle, Proteolytic release of soluble UL16-binding protein 2 from tumor cells. *Cancer Res.* **66**, 2520–2526 (2006). Medline doi:10.1158/0008-5472.CAN-05-2520

8. K. Wiemann, H. W. Mittrücker, U. Feger, S. A. Welte, W. M. Yokoyama, T. Spies, H. G. Rammensee, A. Steinle, Systemic NKG2D down-regulation impairs NK and CD8 T cell responses in vivo. *J. Immunol.* **175**, 720–729 (2005). Medline doi:10.4049/jimmunol.175.2.720

9. M. von Lilienfeld-Toal, S. Frank, C. Leyendecker, S. Feyler, S. Jarmin, R. Morgan, A. Glasmacher, A. Märten, I. G. Schmidt-Wolf, P. Brossart, G. Cook, Reduced immune effector cell NKG2D expression and increased levels of soluble NKG2D ligands in multiple myeloma may not be causally linked. *Cancer Immunol. Immunother.* **59**, 829–839 (2010). Medline doi:10.1007/s00262-009-0807-3

10. N. Guerra, Y. X. Tan, N. T. Joncker, A. Choy, F. Gallardo, N. Xiong, S. Knoblaugh, D. Cado, N. M. Greenberg, D. H. Raulet, NKG2D-deficient mice are defective in tumor surveillance in models of spontaneous malignancy. *Immunity* **28**, 571–580 (2008). Medline doi:10.1016/j.immuni.2008.02.016

11. R. A. Eagle, G. Flack, A. Warford, J. Martínez-Borra, I. Jafferji, J. A. Traherne, M. Ohashi, L. H. Boyle, A. D. Barrow, S. Caillat-Zucman, N. T. Young, J. Trowsdale, Cellular expression, trafficking, and function of two isoforms of human ULBP5/RAET1G. *PLOS ONE* **4**, e4503 (2009). Medline doi:10.1371/journal.pone.0004503

12. M. Xia, N. Guerra, G. K. Sukhova, K. Yang, C. K. Miller, G. P. Shi, D. H. Raulet, N. Xiong, Immune activation resulting from NKG2D/ligand interaction promotes atherosclerosis. *Circulation* **124**, 2933–2943 (2011). Medline doi:10.1161/CIRCULATIONAHA.111.034850

13. L. N. Carayannopoulos, O. V. Naidenko, D. H. Fremont, W. M. Yokoyama, Cutting edge: murine UL16-binding protein-like transcript 1: a newly described transcript encoding a high-affinity ligand for murine NKG2D. *J. Immunol.* **169**, 4079–4083 (2002). Medline doi:10.4049/jimmunol.169.8.4079

14. T. J. Nice, L. Coscoy, D. H. Raulet, Posttranslational regulation of the NKG2D ligand Mult1 in response to cell stress. *J. Exp. Med.* **206**, 287–298 (2009). Medline

15. R. Glas, L. Franksson, C. Une, M. L. Eloranta, C. Ohlén, A. Orn, K. Kärre, Recruitment and activation of natural killer (NK) cells in vivo determined by the target cell phenotype. An adaptive component of NK cell-mediated responses. *J. Exp. Med.* **191**, 129–138 (2000). Medline doi:10.1084/jem.191.1.129

16. A. Diefenbach, E. R. Jensen, A. M. Jamieson, D. H. Raulet, Rae1 and H60 ligands of the NKG2D receptor stimulate tumour immunity. *Nature* **413**, 165–171 (2001). Medline doi:10.1038/35093109

17. D. E. Oppenheim, S. J. Roberts, S. L. Clarke, R. Filler, J. M. Lewis, R. E. Tigelaar, M. Girardi, A. C. Hayday, Sustained localized expression of ligand for the activating NKG2D receptor impairs natural cytotoxicity in vivo and reduces tumor immunosurveillance. *Nat. Immunol.* **6**, 928–937 (2005). Medline doi:10.1038/ni1239

18. C. A. Crane, K. Austgen, K. Haberthur, C. Hofmann, K. W. Moyes, L. Avanesyan, L. Fong, M. J. Campbell, S. Cooper, S. A. Oakes, A. T. Parsa, L. L. Lanier, Immune evasion mediated by tumor-derived lactate dehydrogenase induction of NKG2D ligands on myeloid cells in glioblastoma patients. *Proc. Natl. Acad. Sci. U.S.A.* **111**, 12823–12828 (2014). Medline doi:10.1073/pnas.1413933111

19. N. Nausch, I. E. Galani, E. Schlecker, A. Cerwenka, Mononuclear myeloid-derived "suppressor" cells express RAE-1 and activate natural killer cells. *Blood* **112**, 4080–4089 (2008). Medline doi:10.1182/blood-2008-03-143776

20. J. D. Coudert, L. Scarpellino, F. Gros, E. Vivier, W. Held, Sustained NKG2D engagement induces cross-tolerance of multiple distinct NK cell activation pathways. *Blood* **111**, 3571–3578 (2008). Medline doi:10.1182/blood-2007-07-100057

21. B. Zafirova, S. Mandarić, R. Antulov, A. Krmpotić, H. Jonsson, W. M. Yokoyama, S. Jonjić, B. Polić, Altered NK cell development and enhanced NK cell-mediated resistance to mouse cytomegalovirus in NKG2D-deficient mice. *Immunity* **31**, 270–282 (2009). Medline doi:10.1016/j.immuni.2009.06.017

22. S. Sheppard, C. Triulzi, M. Ardolino, D. Serna, L. Zhang, D. H. Raulet, N. Guerra, Characterization of a novel NKG2D and NKp46 double-mutant mouse reveals subtle variations in the NK cell repertoire. *Blood* **121**, 5025–5033 (2013). Medline doi:10.1182/blood-2012-12-471607

23. M. Ardolino, C. S. Azimi, A. Iannello, T. N. Trevino, L. Horan, L. Zhang, W. Deng, A. M. Ring, S. Fischer, K. C. Garcia, D. H. Raulet, Cytokine therapy reverses NK cell anergy in MHC-deficient tumors. *J. Clin. Invest.* **124**, 4781–4794 (2014). Medline doi:10.1172/JCI74337

24. A. Märten, M. von Lilienfeld-Toal, M. W. Büchler, J. Schmidt, Soluble MIC is elevated in the serum of patients with pancreatic carcinoma diminishing gammadelta T cell cytotoxicity. *Int. J. Cancer* **119**, 2359–2365 (2006). Medline doi:10.1002/ijc.22186

25. A. Clayton, J. P. Mitchell, J. Court, S. Linnane, M. D. Mason, Z. Tabi, Human tumor-derived exosomes down-modulate NKG2D expression. *J. Immunol.* **180**, 7249–7258 (2008). Medline doi:10.4049/jimmunol.180.11.7249

26. O. Ashiru, P. Boutet, L. Fernández-Messina, S. Agüera-González, J. N. Skepper, M. Valés-Gómez, H. T. Reyburn, Natural killer cell cytotoxicity is suppressed by exposure to the human NKG2D ligand MICA*008 that is shed by tumor cells in exosomes. *Cancer Res.* **70**, 481–489 (2010). Medline doi:10.1158/0008-5472.CAN-09-1688

27. R. B. Taylor, W. P. Duffus, M. C. Raff, S. de Petris, Redistribution and pinocytosis of lymphocyte surface immunoglobulin molecules induced by anti-immunoglobulin antibody. *Nat. New Biol.* **233**, 225–229 (1971). Medline doi:10.1038/newbio233225a0

28. E. Narni-Mancinelli, B. N. Jaeger, C. Bernat, A. Fenis, S. Kung, A. De Gassart, S. Mahmood, M. Gut, S. C. Heath, J. Estellé, E. Bertosio, F. Vely, L. N. Gastinel, B. Beutler, B. Malissen, M. Malissen, I. G. Gut, E. Vivier, S. Ugolini, Tuning of natural killer cell reactivity by NKp46 and Helios calibrates T cell responses. *Science* **335**, 344–348 (2012). Medline doi:10.1126/science.1215621

29. A. Iannello, T. W. Thompson, M. Ardolino, S. W. Lowe, D. H. Raulet, p53-dependent chemokine production by senescent tumor cells supports NKG2D-dependent tumor elimination by natural killer cells. *J. Exp. Med.* **210**, 2057–2069 (2013). Medline doi:10.1084/jem.20130783

30. H. Wang, H. Yang, C. S. Shivalila, M. M. Dawlaty, A. W. Cheng, F. Zhang, R. Jaenisch, One-step generation of mice carrying mutations in multiple genes by CRISPR/Cas-mediated genome engineering. *Cell* **153**, 910–918 (2013). Medline doi:10.1016/j.cell.2013.04.025

31. T. J. Nice, W. Deng, L. Coscoy, D. H. Raulet, Stress-regulated targeting of the NKG2D ligand Mult1 by a membrane-associated RING-CH family E3 ligase. *J. Immunol.* **185**, 5369–5376 (2010). Medline doi:10.4049/jimmunol.1000247

32. H. Jung, B. Hsiung, K. Pestal, E. Procyk, D. H. Raulet, RAE-1 ligands for the NKG2D receptor are regulated by E2F transcription factors, which control cell cycle entry. *J. Exp. Med.* **209**, 2409–2422 (2012). Medline doi:10.1084/jem.20120565